MAUSAM, **77**, 2 (April 2026), 657-670

MAUSAM

DOI: https://doi.org/10.54302/mausam.v77i2.6623
Homepage: https://mausamjournal.imd.gov.in/index.php/MAUSAM

UDC No.551.577.13:551.513

Application of machine learning technique and multivariate linear regression for the assessment and prediction of monthly Indian summer monsoon rainfall by using eighteen large-scale circulation indices

RAHUL VERMA* and GANESH D. KALE[1]

**Research Scholar, Department of Civil Engineering*

Sardar Vallabhbhai National Institute of Technology, Surat-395007, Gujarat, India

[1]Associate Professor, Department of Civil Engineering

[1]Sardar Vallabhbhai National Institute of Technology, Surat-395007, Gujarat, India

(*Received 19 October 2024, Accepted 13 June 2025*)

***Corresponding author's email: rahulverma20112@gmail.com**

सार – मासिक भारतीय ग्रीष्मकालीन मॉनसून वर्षा (ISMR) मात्रा कुल ISMR मात्रा से अधिक उपयोगी है। इसलिए, मासिक ISMR के हाइड्रो-क्लाइमैटिक टेलीकनेक्शन (HCT) का आकलन आवश्यक है। समीक्षा किए गए अध्ययनों में से किसी ने भी मासिक ISMR और ग्यारह से अधिक परिसंचरण सूचकांकों के बीच HCT का आकलन नहीं किया है, साथ ही पाँच से अधिक अंतराल भी नहीं पाए हैं। इस प्रकार, वर्तमान अध्ययन में, मासिक ISMR और अठारह परिसंचरण सूचकांकों (प्रत्येक सूचकांक में आठ अंतराल हैं) के बीच HCT का आकलन दो मॉडलों के निर्माण के माध्यम से मल्टीवेरिएट लीनियर रिग्रेशन (MLR) तकनीक और सपोर्ट वेक्टर रिग्रेशन (SVR) नामक मशीन लर्निंग तकनीक को नियोजित करके किया जाता है। वर्तमान अध्ययन में, दो विकास/प्रशिक्षण चरण अवधि 1951-1985 और 1951-1988 माने गए हैं और दो परीक्षण चरण अवधि 1986-2014 और 1989-2014 माने गए हैं जो क्रमशः मॉडल 1 और 2 के हिसाब से हैं, जिनका इस्तेमाल हर तकनीक में किया जाता है। इनिशियल सिग्निफिकेंट लैग्ड सर्कुलेशन इंडेक्स (ISLCIs) लैग्ड सर्कुलेशन इंडेक्स और मासिक ISMR के बीच महत्वपूर्ण सहसंबंधों के आधार पर निकाले जाते हैं। अगर ISLCIs के बीच बहुसंरेखता है तो उसे हटा दिया जाता है ताकि फाइनल सिलेक्टेड सिग्निफिकेंट इंडेक्स (FSSIs) मिल सकें। फिर ISMR के हर माह के लिए मंथली कम्पोजिट इंडेक्स (MCI) को FSSIs और उससे जुड़े मासिक ISMR डेटा का इस्तेमाल करके बनाया जाता है। हर MCI का इस्तेमाल टेस्टिंग फेज़ के दौरान बारिश का अनुमान लगाने के लिए किया जाता है। हर MCI का इस्तेमाल प्रशिक्षण चरण के दौरान वर्षा के पुर्वानुमान के लिए किया जाता है। इसी तरह, SVR टेक्नीक ने दो विकास और प्रशिक्षण चरण से जुड़े FSSIs का इस्तेमाल किया है। अध्ययन में दोनों मॉडलों में कुछ सामान्य FSSI के साथ-साथ मासिक ISMR पर ENSO और EQUINOO के अलावा अन्य परिसंचरण सूचकांकों का प्रभाव भी पाया गया। यह नतीजा निकाला जा सकता है कि SVR तकनिक की प्रगुक्तिक क्षमता MLR तकनिक से ज़्यादा है।

ABSTRACT. The monthly Indian Summer Monsoon Rainfall (ISMR) quantity is more useful than the total ISMR quantity. Therefore, assessment of hydro-climatic teleconnection (HCT) of monthly ISMR is essential. None of the reviewed studies have assessed HCTs between monthly ISMR and more than eleven circulation indices, along with more than five lags. Thus, in the present study, HCTs between monthly ISMR and eighteen circulation indices (each index having eight lags) is assessed by employing the multivariate linear regression (MLR) technique and machine learning technique named support vector regression (SVR) through the formulation of two models. In the present study, two development/training phase periods considered are 1951-1985 and 1951-1988 and two testing phase periods considered are 1986-2014 and 1989-2014 corresponding to models 1 and 2, respectively, which are used in each technique. Initial significant lagged circulation indices (ISLCIs) are derived based on a significant correlation between lagged circulation indices and monthly ISMR. Multi-collinearity amongst ISLCIs is removed, if present, to obtain the significant and independent lagged circulation indices (SILCIs). Then, the monthly composite index (MCI) for every month of the ISMR is developed using SILCIs and corresponding monthly ISMR data. Each MCI is used to forecast rainfall during the

testing phase. Similarly, the SVR technique has used the SILCIs corresponding to the two development and testing phases. The Study found some common SILCIs in both the models along with the effect of circulation indices other than El Nino and Southern Oscillation (ENSO) and Equatorial Indian Ocean Oscillation (EQUINOO) on monthly ISMR. It can be concluded that the predictive power of the SVR technique is more than the MLR technique.

Key words – Hydro-climatic teleconnection, Climatic variability, Indian summer monsoon rainfall, MLR, MCI, SVR.

1. Introduction

Patterns of oceanic/atmospheric teleconnection can influence hydro-climatic phenomena across the globe over large distances. Accurate forecasting of hydro-climatic events (like drought or maximal precipitation events) may aid policymakers in better planning to alleviate negative consequences and take benefit of favorable circumstances. If the link between hydro-climatic events and oceanic and climatic parameters is established, it may be utilized to design an efficient risk management strategy to deal with the extremes of negative consequences (Najafi *et al*., 2022).

Hydrologic variates have a significant link with atmospheric circulation. There are two approaches to model such a link a) simulations executed by the general circulation models (GCMs), and b) assessment of statistical link amongst atmospheric-oceanic variates from various regions of the world and hydrological variables. Such as links called as hydro-climatic teleconnection (HCT) (Singhania *et al*., 2018).

The simulations run by using GCMs show climate change's influence on hydrology and water resources. However, the prospective ability of a GCM declines significantly as it moves from a) hemispheric or continental scale to a local sub-grid scale, b) free troposphere variates to the surface variates, and c) climate-associated variates such as temperature, pressure, humidity, wind and so on to precipitation, soil moisture, runoff and so on, whereas later are more essential for the hydrologic regime (Singhania *et al*., 2018).

Another way of HCT assessment is the evaluation of statistical links amongst hydrologic variates and atmospheric-oceanic variates from various regions of the world, which is computationally less expensive and requires less time and effort. Therefore, this way of HCT assessment is adopted in the present study.

Precipitation is a very crucial parameter for flood warning, hydrological analysis, and water resource management; thus, it is vital to forecast the rainfall precisely (Li *et al*., 2020). For the country's socio-economic gain, the evaluation of the hydro-climatic relationship between various large-scale atmospheric circulations (LACs) and spatiotemporal variability of rainfall is very crucial (Maity and Kumar, 2006). India receives approximately 80% rainfall in the monsoon season; therefore, the Indian summer monsoon (ISM) has a crucial role to play in its social and economic infrastructure. India's economy is dependent on agriculture and its associated industries and it is affected by alteration in ISM (Roy *et al*., 2019). Therefore, assessment of the HCT of ISM is essential.

The studies of HCT between large-scale atmospheric/oceanic circulation indices and precipitation have been carried out outside of India also which are discussed as follows. Karumuri *et al*. (2003) have investigated the impact of Indian Ocean dipole (IOD) on winter rainfall across Australia by using partial correlation. Brandimarte *et al*. (2011) have examined the relationship between North-Atlantic oscillation (NAO) and temperature, river flow, and winter precipitation of the Nile Delta (Egypt) and Southern Italy by employing a cross-correlation technique. Marcella and Eltahir (2008) have studied the interannual, seasonal, and spatial variability of the Kuwait rainfall.

Ionita (2014) had investigated the impact of the East Atlantic/West Russia (EAWR) circulation index on hydro climatology of the Europe from mid-winter to late spring. Najibi *et al*. (2017) have developed a comprehensive framework to assess the flood types, their spatiotemporal characteristics, atmospheric teleconnection, antecedent flow conditions, and causes based on rainfall statistics.

Beurs *et al*. (2018) have formulated one regression model by combining five climate oscillation indices and recognized the importance of each of these indices on land surface phonology, temperature, and precipitation across five countries of Central Asia.

Sehgal and Sridhar (2018) have assessed the interrelationship amongst many climate indices and monthly percentile of soil water storage, potential evapotranspiration, surface runoff, and precipitation for fifty watersheds across the South Atlantic Gulf region of the Southeastern United States for the period 1982-2013. Dehghani *et al*. (2020) have investigated the influence of NAO, Pacific Decadal Oscillation (PDO), and El Nino and Southern Oscillation (ENSO) on seasonal precipitation across Iran. Rasouli *et al*. (2020) have evaluated correlation, and variance and performed singular spectrum analyses to identify the multiple hydroclimatic phases during which climate teleconnection

patterns were related to the hydrology of a small Headwater basin in Idaho, USA. Gao *et al*. (2021) have examined the spatiotemporal variability of rainfall with ENSO and PDO indices in wet and dry seasons across eastern China for the period 1901-2016 by employing principal component analysis (PCA), wavelet coherence, and Bayesian dynamical linear approaches.

Sharma and Teegavarapu (2021) have investigated the impact of two large-scale oceanic/atmospheric oscillations and local hydroclimatology on temperature and seasonal precipitation across Florida. Abel *et al*. (2022) have determined the potential mechanism that influenced precipitation variability by performing PCA on seasonal precipitation of the Southeast Prairie Pothole Region in the U.S.A. Ibebuchi (2023) had investigated the variability patterns of summer rainfall described by land and adjacent oceans in Southern Africa. They have also examined the association between the regionalized rainfall patterns and the modes of climate variability over the South African subcontinent.

Over the past century, many researchers have examined the effect of oceanic/atmospheric circulation indices that affect Indian summer monsoon rainfall (ISMR). Many studies have assessed it for seasonal scale which are discussed as follows. Chang *et al*. (2001) have investigated the inverse association between seasonal ISMR and ENSO. They have found that the relationship has weakened significantly. Chattopadhyay and Bhatla (2002) have examined the association between the all-India monsoon rainfall and sea-surface temperature (SST) anomalies over several Nino regions of the equatorial Pacific Ocean for the period 1949-1995. They have also grouped the SST and seasonal rainfall according to the Quasi-Biennial Oscillation (QBO) phases at the 50-hPa.

Gadgil *et al*. (2004) have studied the relationship of the seasonal ISMR with a linearly combined index made up of seasonally averaged Equatorial Indian Ocean Oscillation (EQUINOO) and ENSO of all seasons. Ihara *et al*. (2007) have examined the association between the state of the equatorial Indian Ocean, ENSO, and seasonal ISMR for the period 1881-1998 by using multiple regression analysis.

Peings *et al*. (2009) have proposed a Pacific North America (PNA) related index which was strongly correlated with the subsequent seasonal ISMR. Boschat *et al*. (2012) have investigated the linear association between global SST anomalies and seasonal ISMR for the periods 1950-1976 and 1979-2006. Mishra *et al*. (2012) have examined the dominant patterns of seasonal ISMR and their association with 850-hpa wind fields and SST by employing gridded datasets for the period 1900 on.

Srivastava *et al*. (2019) have investigated that the ENSO-ISMR association was weakened over the previous seven decades. Yang and Huang (2021) have investigated the restored ENSO-ISMR association since 1999/2000 by using 19- and 21-year sliding correlation for the period of 1871- 2019.

Sardana *et al*. (2022) have examined the independent and complete impact of IOD by employing dipole mode index (DMI) and ENSO by employing Nino 3, Nino 3.4, and Nino 4 on seasonal extreme and mean surface air temperature over India and ISMR. Athira *et al*. (2023) have investigated the alteration in the association between the seasonal ISMR and ENSO. They have examined how this association is influenced by the major drivers of ISMR.

For reservoir operations, crop planning, water distribution to various users, and other purposes, the monthly rainfall quantity of a given month is more useful than the total monsoon rainfall quantity (Singhania *et al*., 2018). Therefore, assessment of HCT of monthly ISMR is essential.

Many researchers have assessed HCTs of monthly ISMR which are discussed as follows. Karumuri *et al*. (2001) have studied the influence of the IOD on the association between the ENSO and monthly ISMR by using Monte-Carlo simulations and correlation. The study demonstrated that the effect of IOD events on ISMR is on their own and therefore strengthens and weakens the effect of ENSO on ISMR.

Srivastava *et al*. (2002) have investigated the connection between the outgoing longwave radiation (OLR) and SST anomalies over the Atlantic Ocean with monthly ISMR. The study showed that there were statistically significant relationships between ISMR and OLR and SST anomalies across the North Atlantic Ocean for May month, which were indicators of the NAO.

Maity and Kumar (2006) have examined the impact of EQUINOO and ENSO on monthly ISMR by developing a monthly composite index (MCI) while considering a lagged relationship. Also, they have investigated the spatial variability of this relationship for different homogeneous regions of India. The study found that the predictability of monthly ISMR was aided by employing MCI.

Karumuri and Saji (2007) have examined the relative effect of IOD and ENSO on monthly ISMR at a sub-regional scale by applying partial correlation and multiple regression techniques. The significant impact of IOD and

ENSO events was observed on monthly ISMR across several parts of India. Maity *et al.* (2007) have investigated the impact of EQUINOO and ENSO on monthly ISMR by employing correlation and partial correlation by considering five lags (0 to 4). They have examined the combined effect of ENSO and IOD, IOD alone and ENSO alone on ISMR. The study found that, monthly rainfall of all India was dependent on the relative dominance of EQUINOO and ENSO indices.

Singhania *et al*. (2018) have used eleven indices (each with four lags) and derived significant and independent lagged circulation indices (SILCIs) influencing monthly ISMR by removing multi-collinearity existing amongst the SLCIs and formulating MCIs. The 4 models were developed corresponding to model development phase periods viz. 1950 to 1999, 1950 to 1994, 1950 to 1989, and 1950 to 1984. The MCIs formulated for ISMR months corresponding to each of the 4 models were used for forecasting the rainfall for the common time interval 2000 to 2014. In this study, MCIs corresponding to monthly ISMR were formulated with the help of SILCIs and these MCIs were found to be changing with time, having some uncommon indices and some common indices.

Feba *et al*. (2019) have examined the decadal variability of teleconnection amongst the ENSO and monthly ISMR over the period of 1958 to 2008. The significance of the correlation was ascertained between monthly ISMR and two NINO indices by employing a bootstrapping test. The teleconnection between ENSO and ISMR was found to be weak.

For the assessment of HCT of ISMR, multivariate linear regression (MLR) was used by few studies (Maity and Kumar 2006; Ihara *et al*. 2007; Karumuri and Saji 2007; Peings *et al*. 2009; Singhania *et al*. 2018). None of the reviewed studies have assessed HCTs between monthly ISMR and circulation indices by using a machine-learning (ML) technique named support vector regression (SVR) with a linear kernel function.

Among aforesaid studies, only one study performed by Singhania *et al*. (2018) had executed removal of multi-collinearity among initial significant lagged circulation indices (ISLCIs) to select the SILCIs. It is worth noting that, none of the reviewed studies have assessed HCTs between monthly ISMR with more than eleven circulation indices, along with more than five lags.

Thus, in this study, HCT between 144 lagged circulation indices and monthly ISMR is assessed by using the MCIs formulated by using the MLR technique. MCIs are formulated after the removal of multi-collinearity present between selected significant inputs. These MCIs are formulated for two models corresponding to two development phase periods viz. 1951-1985 and 1951-1988. The ability of generated MCIs to forecast monthly ISMR is examined by evaluating the correlation between observed and forecasted rainfall in the testing phases 1986-2014 and 1989-2014 for MLR model 1 and MLR model 2, respectively. Similarly, the SVR model is developed by using SILCIs (inputs) and corresponding monthly ISMR (target output) for SVR model 1 and SVR model 2 corresponding to training phase periods 1951-1985 and 1951-1988, respectively. The predictive power of SVR is assessed by estimating the correlation coefficient between observed and corresponding predicted rainfall during the testing phases of 1986-2014 and 1989-2014 for SVR Model 1 and SVR Model 2, respectively.

2. Data and methodology

2.1. *Data*

The dataset of 18 circulation indices (with eight lags for every index) is used in the study. These indices are given in the Table 1 with the corresponding sources. Monthly ISMR data (All India monthly data of monsoon months) is also used in the study.

2.2. *Methodology*

2.2.1. *Methodology for the development of MCI*

The methodology used in the current study is referred from Singhania *et al*. (2018). To investigate the temporal variation of the HCTs present amongst 144 lagged circulation indices and monthly ISMR, two different models are prepared. Each model consisted of a development and testing phase.

In each model, a significant correlation at a 5% significance level is determined amongst the 144 lagged circulation indices and monthly ISMR. The LCIs that have a significant correlation with the target output (monthly ISMR) are selected which are called ISLCIs. The multi-collinearity present amongst these ISLCIs is eliminated, if present. Suppose, if multi-collinearity is present amongst two ISLCIs then multi-collinearity is removed by keeping that index which has a higher significant correlation with the respective target output *i.e.*, given monthly ISMR and removing another index. The remaining indices after removing the multi-collinearity amongst the ISLCIs are called as SILCIs. SILCIs are employed further in the formulation of MCI by employing MLR corresponding to each monthly ISMR. The ability of generated MCIs to forecast monthly ISMR is examined by evaluating the correlation between observed and forecasted rainfall in the testing phase.

TABLE 1

Rainfall and oceanic/atmospheric circulation indices data used in the study

Sr. No.	Data	Sources of data
	Rainfall	
1.	All India Monthly rainfall data	https://www.tropmet.res.in/data/data-archival/rain/iitm-regionrf.txt
	Oceanic/Atmospheric Circulation Indices	
1	Arctic Oscillation (AO) index	Sources are referred and sources are available in Singhania *et al*. (2018)
2	East Atlantic (EA) index	
3	East Atlantic-West Russia (EAWR) index	
4	El Nino/Southern Oscillation (ENSO) index	
5	EQWIN index	
6	North Atlantic Oscillation (NAO) index	
7	Pacific Decadal Oscillation (PDO) index	
8	(Pacific-North American) PNA index	
9	Scandinavia (SCAND) - index	
10	West Pacific (WP)	
11	Interdecadal Pacific oscillation (IPO)	https://psl.noaa.gov/data/timeseries/IPOTPI/
12	Antarctic oscillation (AAO)	https://psl.noaa.gov/data/20thC_Rean/timeseries/monthly/AAO/
13	Atlantic multidecadal oscillation (AMO)	https://psl.noaa.gov/data/correlation/amon.us.long.data
14	Caribbean Index (CAR)	https://psl.noaa.gov/data/correlation/CAR_ersst.data
15	North Pacific Index (NP)	https://psl.noaa.gov/data/20thC_Rean/timeseries/monthly/NP/np.20crv2c.long.data
16	Polar/ Eurasia (POL)	https://www.cpc.ncep.noaa.gov/data/teledoc/poleur.shtml
17	Tropical Northern Atlantic (TNA) index	https://psl.noaa.gov/data/correlation/tna.data
18	Tropical Southern Atlantic (TSA) Index	https://psl.noaa.gov/data/correlation/tsa.data

The SILCIs are further employed in SVR models corresponding to the same training and testing phases as that of MLR models.

TABLE 2

Different development and testing phases used corresponding to two models correspondent to two techniques for assessment of HCTs between 144 lagged circulation indices with their successive number of lags and monthly ISMR

Model	Development/Training phase	Testing phase	Number of circulation indices	Number of lags	Number of inputs
1	1951-1985	1986-2014	18	8	144
2	1951-1988	1989-2014	18	8	144

Two models having two different development and testing phases are used for the assessment of HCTs between 144 lagged circulation indices and monthly ISMR for generating MCIs, which are given in Table 2. Similarly, two different models are formed by using the SVR approach corresponding to the same training and testing phases as of MLR models.

Since the 1950s, there has been an extensive decrease in the continental diurnal temperature range (DTR), which corresponds to an increase in the quantity of clouds (Singhania *et al*., 2018). Considering the starting year of the model from 1950 will lead to including the indices from the year 1949 (for example- for June month ISMR, 8 lags are October, November, December, January, February, March, April, and May), which is not feasible for few indices because of unavailability of data. Thus, in the present study, the starting year is considered as 1951 for both models. So, the common starting period has to be considered as 1951. Maity and Kumar (2007) utilized a 35-year sliding window to evaluate various coefficients of MCI equations and discovered that they are almost stable with very little fluctuation. So, in the present study, the duration of both models (1951-1985 and 1951-1988) is either 35 years or more.

The methodology is illustrated in the Fig. 1.

Monthly Composite Index (MCI)

The MCI is formed to investigate its relationship with monthly fluctuations of the ISMR.

Correlated past month indices were used to form MCI (Maity and Kumar, 2006).

$$\text{MCI of monthly ISMR} = C_1 Ind_1 + C_2 Ind_2 \quad (1)$$

where, C_1 and C_2 are coefficients, while Ind_1 and Ind_2 are circulation indices.

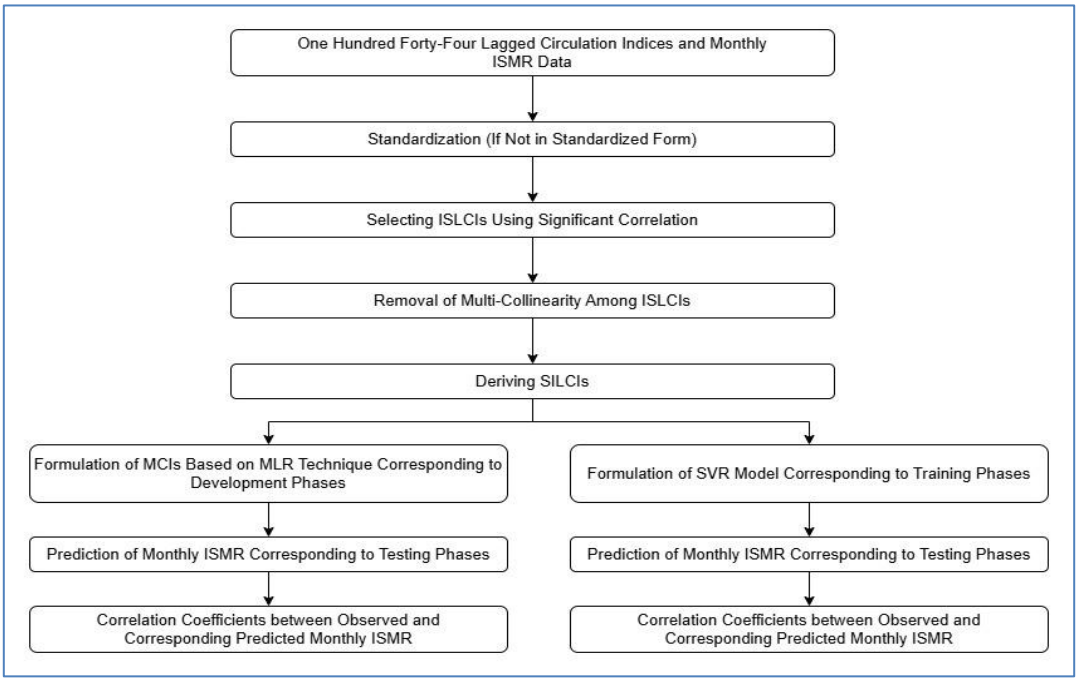

Fig. 1. Methodology flow-chart

In the present study, MCI is formed amongst monthly ISMR and SILCIs by employing MLR technique.

Support Vector Regression (SVR)

Support Vector Machine (SVM) is one of the supervised learning models used for both regression and classification tasks. SVM for regression is specifically known as SVR. SVR can be either linear or non-linear, depending on the chosen kernel function (Kavitha *et al*., 2016).

Linear Support Vector Regression

SVR employs linear kernel functions for the regression similar to SVMs. However, unlike SVM, SVR sets a tolerance margin (ε) to allow for approximation. Equation 2 describes the SVR equation formed by using a linear kernel function (Kavitha *et al*., 2016).

$$y = \mathrm{w.x} + \mathrm{b} \qquad (2)$$

where, y = input space,
w. x = vector product,
b = constant.

Based on the error function in equation 3, it can be minimized such that the target becomes z_i.

$$min\frac{1}{2}\|w^2\| + c\sum_{i=1}^{n}(\xi_i + \xi_i^*) \qquad (3)$$

subjected to

$$\begin{cases} z_i - (\mathrm{w.x} + \mathrm{b}) & \leq \varepsilon + \xi_i \\ (w.x) + b - z_i & \leq \varepsilon + \xi_i^* \\ \xi_i \xi_i^* & \geq 0 \end{cases}$$

3. Results and discussion

In the following section, the results of MLR and SVR models are shown. Later the discussion section is provided to highlight the findings.

3.1. *MLR and SVR Models*

HCTs between 144 lagged circulation indices and monthly ISMR are aSssessed in the present study through the formulation of two models corresponding to each of the MLR and SVR approaches. The MLR and SVR models have the same development/training phases and testing phases.

3.2. *Results of model 1*

3.2.1. *Results of MLR Model 1:*

(i) *Deriving ISLCIs and SILCIs for the development phase (1951-1985) of model 1:*

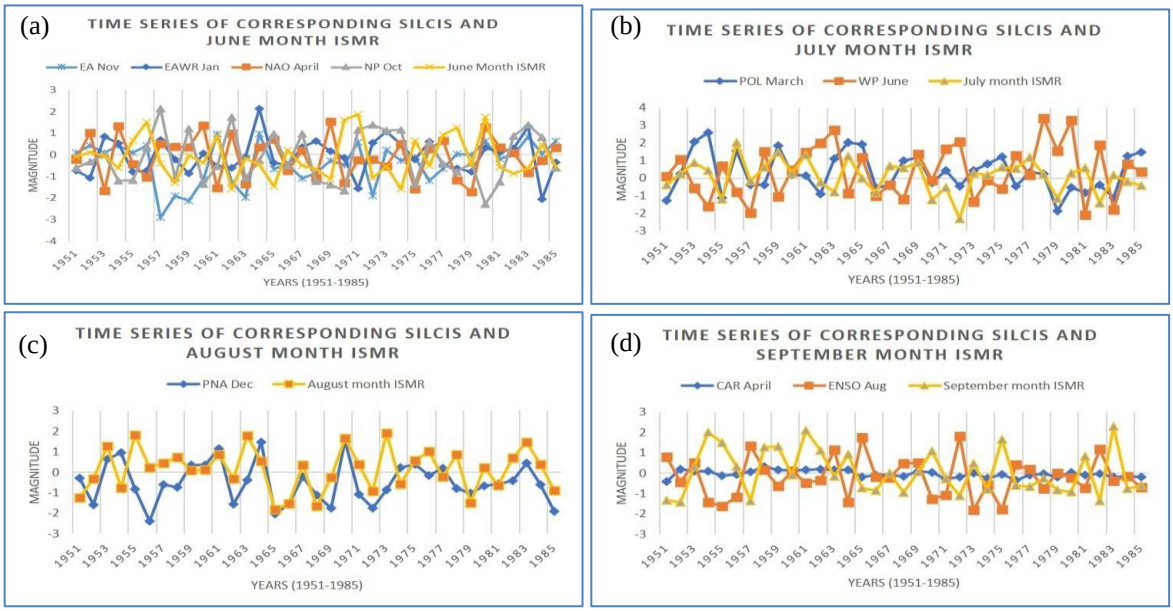

Figs. 2(a-d). Time series of corresponding SILCIs with a) June month rainfall, b) July month rainfall c) August month rainfall, d) September month rainfall

TABLE 3

ISLCIs for monthly ISMR before removal of multi-collinearity for model 1's development phase (1951-1985)

Sr. No.	Months of ISMR	ISLCIs Before Removal of Multi-collinearity
1	June	AO_{April} EA_{Nov} $EAWR_{Jan}$ NAO_{April} NP_{Oct} PNA_{April}
2	July	CAR_{May} EA_{March} $EQWIN_{Dec}$ PNA_{Feb} POL_{March} WP_{June}
3	August	NP_{Dec} PNA_{Dec}
4	September	AMO_{March} CAR_{March} CAR_{April} CAR_{May} EA_{April} $EAWR_{Aug}$ $ENSO_{Jan}$ $ENSO_{Feb}$ $ENSO_{Aug}$ IPO_{July} IPO_{Aug}

The LCIs having a significant correlation (at a 5% significance level) with target output (monthly ISMR) are selected first and these are called as ISLCIs. The ISLCIs selected for monthly ISMR corresponding to four months *viz*. June, July, August, and September and model 1's development phase (1951-1985) are shown in Table 3.

The multi-collinearity found amongst ISLCIs is removed for each monthly ISMR. The SILCIs after the removal of multi-collinearity are presented in Table 4.

The time series of SILCIs with respective monthly ISMR for model 1's development phase (1951-1985) are shown in the Fig. 2.

It can be observed clearly from the above Fig. 2 that, the temporal evolution of SILCIs and monthly ISMR are coherent corresponding to the development phase of model 1.

(ii) *Formulation of MCIs for monthly ISMR corresponding to MLR model 1*

MCI is formed amongst SILCIs and corresponding monthly ISMR by using a MLR approach. The MCIs for monthly ISMR for model 1's development phase (1951-1985) are shown in the Table 5. Correlation coefficients between observed and predicted rainfall for monthly ISMR corresponding to MLR model 1's development phase (1951-1985) are also shown in Table 5.

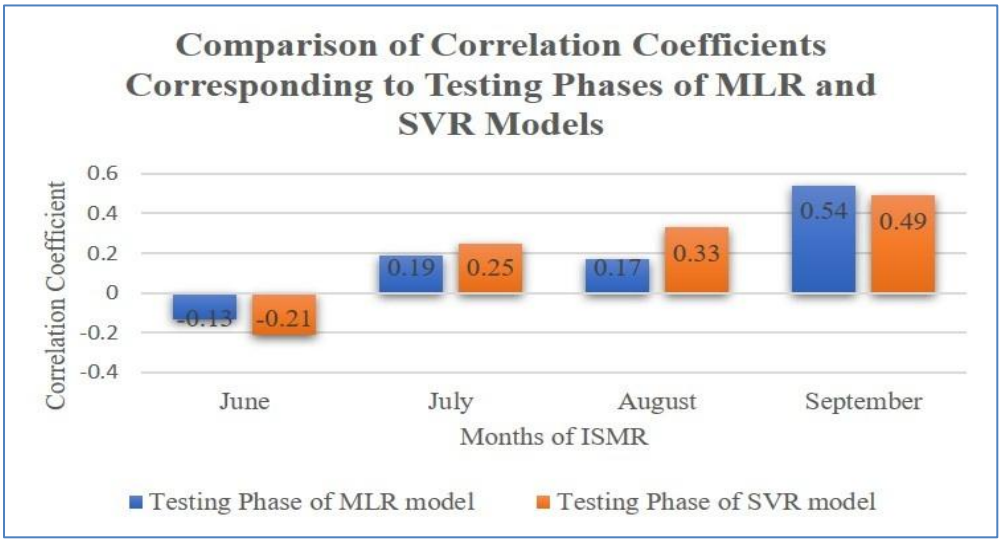

Fig. 3. Correlation coefficients estimated between observed and corresponding predicted monthly ISMR correspondent to testing phases of MLR model 1 and SVR model 1

TABLE 4

SILCIs derived for monthly ISMR after removal of multi-collinearity for model 1's development phase (1951-1985)

Sr. No.	Months of ISMR	Significant Inputs After Removal of Multi-collinearity
1.	June	EA_{Nov} $EAWR_{Jan}$ NAO_{April} NP_{Oct}
2.	July	POL_{March} WP_{June}
3.	August	PNA_{Dec}
4.	September	CAR_{April} $ENSO_{Aug}$

TABLE 5

MCIs for monthly ISMR for MLR model 1's development phase (1951-1985)

Sr. No.	Months of ISMR	MCIs	R
1.	June	$Rain_{June} = -0.0999 + 0.2460 * EA_{Nov} - 0.4231 * EAWR_{Jan} - 0.2792 * NAO_{April} - 0.1987 * NP_{Oct}$	0.65
2.	July	$Rain_{July} = 0.0530 + 0.3526 * POL_{March} - 0.1544 * WP_{June}$	0.54
3.	August	$Rain_{August} = 0.3564 + 0.4436 * PNA_{Dec}$	0.43
4.	September	$Rain_{September} = 0.0147 + 2.0708 * CAR_{April} - 0.6366 * ENSO_{Aug}$	0.67

The correlation coefficients corresponding to the June to September months are 0.65, 0.54, 0.43, and 0.67, respectively.

Testing Phase of MLR Model 1

MCIs developed for monthly ISMR corresponding to the development phase of MLR model 1 are shown in Table 5 and these MCIs are utilized to forecast the corresponding rainfall for the testing period of 1986-2014. The correlation is evaluated amongst observed and predicted rainfall for every month of ISMR corresponding to the testing phase period 1986-2014, and Table 6 shows the values of these correlation coefficients.

3.2.2 *Results of SVR Model 1*

The HCTs between monthly ISMR and 144 lagged circulation indices is assessed by using the SVR technique with a linear kernel function. SILCIs presented in Table 4 are used for formulating the SVR models. The training period for the SVR model is the same as that of MLR model 1 (*i.e.*, 1951-1985). Similarly, the predictive potential of the SVR model is investigated for the testing phase period (*i.e.*, 1986-2014). Table 7 presents the correlation coefficients between observed and corresponding predicted monthly ISMR corresponding to training and testing phase periods for SVR model 1.

Fig. 3 shows the correlation coefficients estimated between observed and corresponding predicted monthly ISMR correspondent to the testing phases of MLR model 1 and SVR model 1.

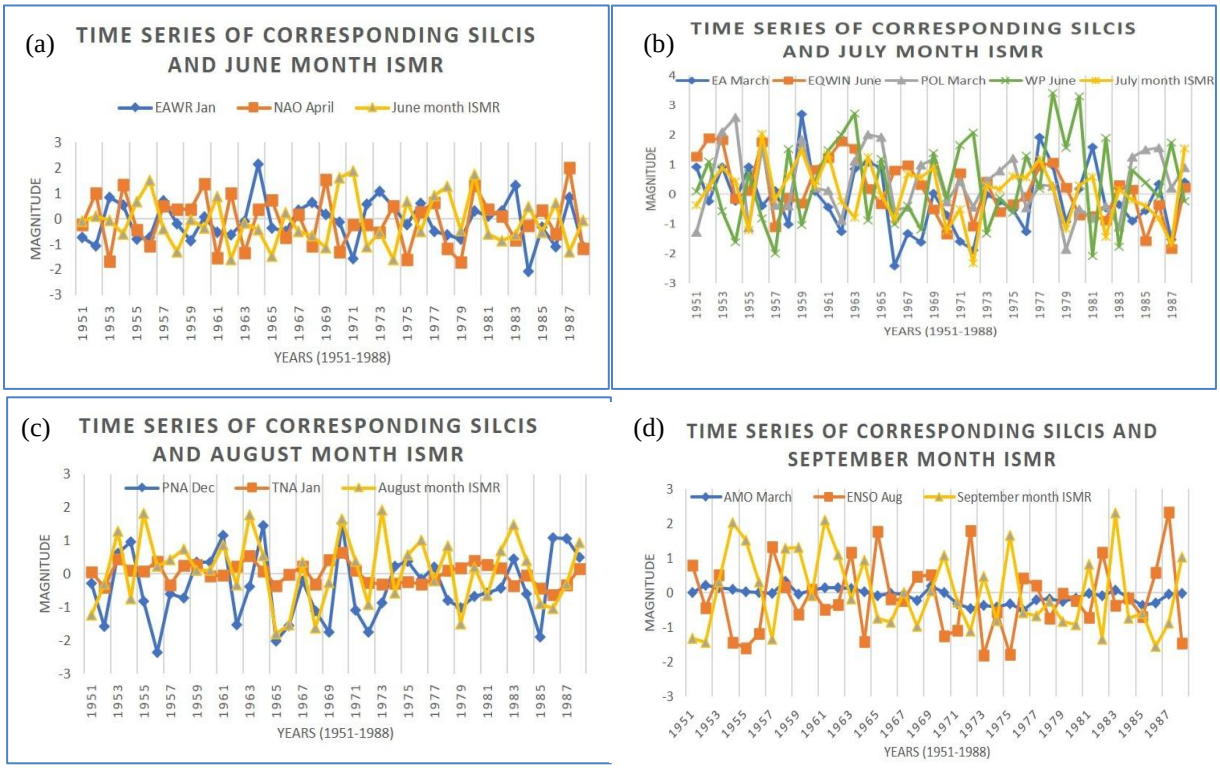

Figs. 4(a-d). Time series of corresponding SILCIs with a) June month rainfall, b) July month rainfall c) August month rainfall, and d) September month rainfall

TABLE 6

Correlation coefficients estimated corresponding to monthly ISMR for the testing phase (1986-2014) of MLR model 1

Sr. No.	Months of ISMR	Correlation Coefficient
1.	June	-0.13
2.	July	0.19
3.	August	0.17
4.	September	0.54

TABLE 7

Correlation coefficients estimated between observed and corresponding predicted monthly ISMR correspondent to training and testing phase periods for SVR model 1

Sr. No.	Months of ISMR	Correlation Coefficient corresponding to the training phase	Correlation Coefficient corresponding to the testing phase
1.	June	0.40	-0.21
2.	July	0.42	0.25
3.	August	0.19	0.33
4.	September	0.71	0.49

3.3 *Results of Model 2*

3.3.1. Results of MLR Model 2

(i) Deriving ISLCIs and SILCIs for the development phase (1951-1988) of model 2:

ISLCIs are derived based on a statistically significant correlation between LCIs and monthly ISMR at a 5% significance level. The ISLCIs for monthly ISMR corresponding to four months viz. June, July, August, and September and model 2's development phase (1951-1988) are presented in Table 8.

The multi-collinearity found amongst ISLCIs is removed for every month of ISMR. The SILCIs derived after eliminating the multi-collinearity are presented in Table 9.

The time series of SILCIs with respective monthly ISMR for model 2's development phase (1951-1988) are shown in the Fig. 4.

It can be observed clearly from the above Fig. 4 that, the temporal evolution of SILCIs and monthly ISMR are coherent corresponding to the development phase of model 2.

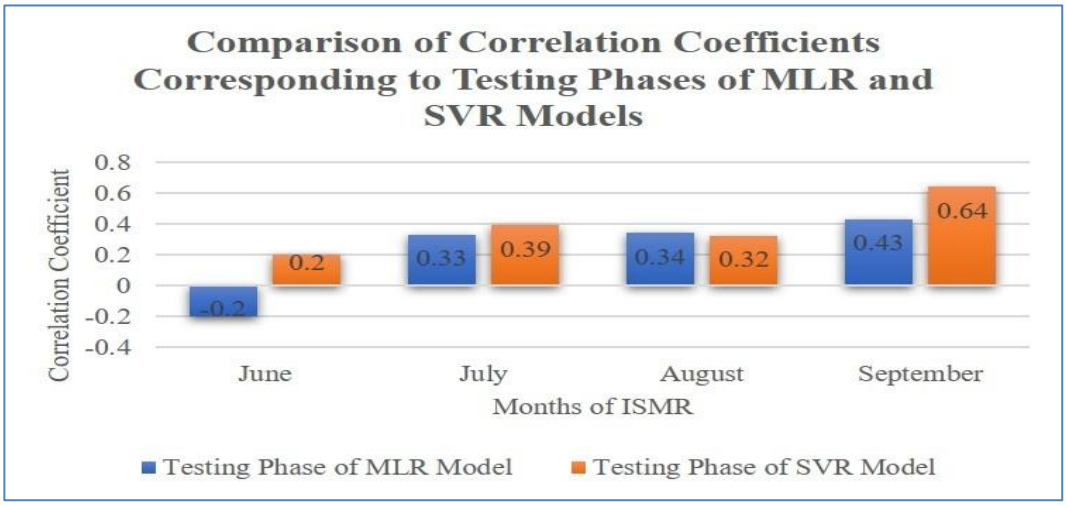

Fig. 5. Correlation coefficients estimated between observed and corresponding predicted monthly ISMR correspondent to testing phases of MLR model 2 and SVR model 2

TABLE 8

ISLCIs for monthly ISMR before removal of multi-collinearity for model 2's development phase (1951-1988)

Sr. No.	Months of ISMR	ISLCIs Before Removal of Multi-collinearity
1	June	AO_{April} $EAWR_{Jan}$ $EQWIN_{Nov}$ $EQWIN_{March}$ NAO_{April}
2	July	AMO_{Nov} AO_{Nov} CAR_{May} EA_{March} $EQWIN_{June}$ POL_{March} TNA_{Nov} WP_{June}
3	August	CAR_{April} PNA_{Dec} TNA_{Jan}
4	September	AMO_{March} AMO_{April} CAR_{March} CAR_{April} CAR_{May} EA_{April} $EAWR_{Aug}$ $ENSO_{Jan}$ $ENSO_{June}$ $ENSO_{Aug}$ $EQWIN_{July}$ IPO_{July} IPO_{Aug} TNA_{Jan} TNA_{Feb} TNA_{March}

TABLE 9

SILCIs derived for monthly ISMR after removal of multi-collinearity for model 2's development phase (1951-1988)

Sr. No.	Months of ISMR	SILCIs for Every Month of ISMR
1.	June	$EAWR_{Jan}$ NAO_{April}
2.	July	EA_{March} $EQWIN_{June}$ POL_{March} WP_{June}
3.	August	PNA_{Dec} TNA_{Jan}
4.	September	AMO_{March} $ENSO_{Aug}$

(ii) Formulation of MCI for monthly ISMR corresponding to MLR model 2

MCI is formed amongst SILCIs and corresponding monthly ISMR by using an MLR approach. The MCIs for monthly ISMR for MLR model 2's development phase (1951-1988) are shown in Table 10. Correlation coefficients between observed and corresponding predicted rainfall for monthly ISMR corresponding to MLR model 2's development phase (1951-1988) are also shown in Table 10. The correlation coefficients corresponding to the June to September months are 0.55, 0.63, 0.34, and 0.73, respectively.

(iv) Testing Phase corresponding to MLR model 2

MCIs developed for monthly ISMR corresponding to the development phase of MLR model 2 are shown in

TABLE 10

MCIs for monthly ISMR for the period 1951-1988 for MLR model 2

Sr. No.	Months of ISMR	MCIs	R
1.	June	$Rain_{June}$ = -0.1931 – 0.4187* $EAWR_{Jan}$ – 0.3162* NAO_{April}	0.55
2.	July	$Rain_{July}$ = -0.0633 + 0.2374* EA_{March} + 0.3633* $EQWIN_{June}$ + 0.3068* POL_{March} – 0.1859* WP_{June}	0.63
3.	August	$Rain_{August}$ = 0.2329 + 0.3260* PNA_{Dec} + 1.0668* TNA_{Jan}	0.34
4.	September	$Rain_{September}$ = 0.0960 + 2.2253* AMO_{March} – 0.6584* $ENSO_{Aug}$	0.73

TABLE 11

Correlation coefficients estimated corresponding to monthly ISMR for the testing phase (1989-2014) of MLR model 2

Sr. No.	Months of ISMR	Correlation Coefficient
1.	June	-0.20
2.	July	0.33
3.	August	0.34
4.	September	0.43

Table 10 and these MCIs are utilized to forecast the corresponding rainfall for the testing phase period of 1989-2014. The correlation is estimated amongst observed rainfall and predicted rainfall for every month of ISMR corresponding to the testing phase period 1989-2014 and Table 11 shows values of these correlation coefficients.

3.3.2 *Results of SVR Model 2*

The HCTs between monthly ISMR and 144 lagged circulation indices is assessed by using the SVR technique with a linear kernel function. SILCIs presented in Table 9 are used for formulating SVR model 2. The training period for SVR model 2 is the same as for MLR model 2 (*i.e.*, 1951-1988). Similarly, the predictive potential of the SVR model is investigated for the testing phase period (*i.e.*, 1989-2014). Table 12 presents the correlation coefficients between observed and corresponding predicted monthly ISMR correspondent to training and testing phase periods for SVR model 2.

Fig. 5 shows the correlation coefficients estimated between observed and corresponding predicted monthly ISMR correspondent to the testing phases of MLR model 2 and SVR model 2.

TABLE 12

Correlation coefficients estimated between observed and corresponding predicted monthly ISMR correspondent to training and testing phase periods for SVR model 2

Sr. No.	Months of ISMR	Correlation Coefficient corresponding to the training phase	Correlation Coefficient corresponding to the testing phase
1.	June	0.15	0.20
2.	July	0.64	0.39
3.	August	0.36	0.32
4.	September	0.65	0.64

3.4.1. *Discussion*

For June month ISMR corresponding to model 1, EA_{Nov}, $EAWR_{Jan}$, NAO_{April}, and NP_{Oct} are found to be significant inputs. Singhania *et al*. (2018) have also found NAO_{April} as SILCI for June month ISMR corresponding to the development phase of model 4 (35 years) as found in the present study. Also, Srivastava *et al*. (2002) have also shown a strong association between NAO and monthly ISMR. For July month ISMR, corresponding to model 1, POL_{March}, and WP_{June} are found to be statistically significant inputs. For August month ISMR corresponding to model 1, PNA_{Dec} is found to be a significant input. For September month ISMR corresponding to model 1, CAR_{April}, and $ENSO_{Aug}$ are found to be statistically significant inputs. Singhania *et al*. (2018) have also found $ENSO_{Aug}$ as SILCI for September month ISMR corresponding to the development phase of model 4 (35 years) as in the present study. There are new SILCIs found in the present study that are not found by Singhania *et al*. (2018), for June month ISMR, these new SILCIs are EA_{Nov}, $EAWR_{Jan}$ and NP_{Oct}; for July month ISMR, new SILCIs are POL_{March} and WP_{June}; for August month ISMR, new SILCI is PNA_{Dec} and for September month ISMR, new SILCI is CAR_{April} corresponding to model 1.

Correlation coefficients for monthly ISMR of June, July, August, and September corresponding to the testing phase of MLR model 1 are -0.13, 0.19, 0.17, and 0.54 and these for the testing phase of model 4 in Singhania *et al*. (2018) are -0.01, 0.06, 0.21 and 0.42. Correlation coefficients for monthly ISMR of June, July, August, and September corresponding to the testing phase of SVR model 1 are -0.21, 0.25, 0.33, 0.49. A comparison of the testing phase results of the present study (MLR model 1) and testing phase results obtained for model 4 in Singhania *et al*. (2018) shows that the results obtained in the present study are better in majority cases.

For June month ISMR corresponding to model 2, $EAWR_{Jan}$, and NAO_{April} are found to be significant inputs. Singhania *et al*. (2018) have also found NAO_{April} as SILCI for June month ISMR corresponding to the development phase of model 3 (40 years) as found in the present study. Srivastava *et al*. (2002) have also shown a strong association between NAO and monthly ISMR. For July month ISMR, corresponding to model 2, EA_{March}, $EQWIN_{June}$, POL_{March}, and WP_{June} are derived as SILCIs. Singhania *et al*. (2018) have also found $EQWIN_{June}$ and WP_{June} as SILCI for July month ISMR corresponding to the development phase of model 3 (40 years) as found in the present study. For August month ISMR corresponding to model 2, PNA_{Dec}, and TNA_{Jan} are found to be significant inputs. Peings *et al*. (2009) have shown a strong relationship between the PNA-related index and monthly ISMR which supports the result obtained in the present study for August month ISMR corresponding to model 2. For September month ISMR corresponding to model 2, AMO_{March}, and $ENSO_{Aug}$ are found to be significant inputs. Singhania *et al*. (2018) have also found $ENSO_{Aug}$ as SILCI for September month ISMR corresponding to the development phase of model 3 (40 years) as found in the present study. New SILCIs found in the present study but not found by Singhania *et al*. (2018) are $EAWR_{Jan}$ for June month ISMR; POL_{March} for July month ISMR; PNA_{Dec}, and TNA_{Jan} for August month ISMR and AMO_{March} for September month ISMR corresponding to model 2. Correlation coefficients for monthly ISMR of June, July, August, and September corresponding to the testing phase of MLR model 2 are -0.20, 0.33, 0.34, 0.43 and these for the testing phase of model 3 in Singhania *et al*. (2018) are 0.20, 0.064, 0.21, and 0.49. Correlation coefficients for monthly ISMR of June, July, August, and September corresponding to the testing phase of SVR model 2 are 0.20, 0.39, 0.32, 0.64. A comparison of the testing phase results of MLR model 2 in the present study and the testing phase results obtained for model 3 in Singhania *et al*. (2018) shows that the results obtained in the present study for majority cases are better. It is also worth noting that, HCTs between monthly ISMR and SILCIs are changing over time.

Teleconnections, NAO, ENSO, IOD, etc. are frequently studied in their mature phase of variability, with the understanding that teleconnections evolve on a spatiotemporal scale. However, because natural systems are inherently complex, identifying patterns and relationships has always been difficult. When combined with the current problems of global warming-induced climate change, these interactions and patterns become even more unexpected, unpredictable and usual. With these challenging facts, climate science investigations worldwide understand that climatic and other geophysical phenomena are essentially nonlinear, carrying multiscale characteristics and impacts that are typically time varying. (Agarwal *et al*., 2022). This is the reason why HCT varies with time as found in the present study.

4. Conclusions

In the present study, the HCTs between monthly ISMR and 144 lagged circulation indices is assessed by using two development phase periods viz., 1951-1985 and 1951-1988, and two testing phase periods 1986-2014 and 1989-2014 corresponding to MLR and SVR model 1 and 2, respectively. ISLCIs are derived based on a significant correlation (5% significance level) between the LCIs and monthly ISMR (target output). Multi-collinearity amongst ISLCIs is removed to obtain SILCIs. Then, MCIs for monthly ISMR are formulated between SILCIs and corresponding observed monthly ISMR data which are used for forecasting rainfall in the testing phase.

The conclusions drawn from the current study are as follows:

(i) HCTs assessment between monthly ISMR and 144 lagged circulation indices have shown better results as compared to that performed by using eleven circulation indices (each index having four lags) in Singhania *et al*. (2018).

(ii) The study found, some common SILCIs in both the models along with the effect of circulation indices other than ENSO and EQUINOO on monthly ISMR as found in Singhania *et al*. (2018).

(iii) There are new SILCIs found in the present study that are not found by Singhania *et al*. (2018), for June month ISMR, these new SILCIs are EA_{Nov}, $EAWR_{Jan}$ and NP_{Oct}; for July month ISMR, new SILCIs are POL_{March} and WP_{June}; for August month ISMR, new SILCI is PNA_{Dec} and for September month ISMR, new SILCI is CAR_{April} corresponding to model 1. Similarly for model 2, new SILCIs found in the present study but not found by Singhania *et al*. (2018) are $EAWR_{Jan}$ for June month ISMR; POL_{March} for July month ISMR; PNA_{Dec}, and TNA_{Jan} for August month ISMR and AMO_{March} for September month ISMR.

(iv) Many SILCIs derived in the present study corresponding to monthly ISMR are also obtained in the previous studies which supports the results of the current study.

(v) Results obtained for the testing phase are better as compared to those presented by Singhania *et al*. (2018).

(vi) MLR and SVR models presented in the study show that the HCTs of monthly ISMR change with respect to time.

(vii) It is seen that the SVR technique has performed better than the MLR technique.

Acknowledgements

The authors are thankful to the Indian Institute of Tropical Meteorology, Pune, and the National Oceanic and Atmospheric Administration, USA for providing all relevant data through their portal, which is used in the current study.

Data Availability

The sources of the obtained data are mentioned in the subsection 2.1 dataset.

Authors' Contributions

Rahul Verma: Data collection, Analysis and Preparation of the Draft. (*email-rahulverma20112@gmail.com*)
Ganesh D. Kale: Conceptualization, Supervision, and Editing. (*email-gdk@ced.svnit.ac.in*)

Disclaimer: The views and contents expressed in this study are the views of the authors and do not necessarily reflect the views of the organizations they belong to.

References

Abel, B. D., Rajagopalan, B. and Ray, A. J., 2022, "Space–Time Variability of Summer Hydroclimate in the US Prairie Pothole Region", *Earth Interactions*, **26,** 1, 39-51.

Agarwal, A., Yuan, N., Cheung, K. K. and Shukla, R., 2022, "Emerging hydro-climatic patterns, teleconnections, and extreme events in changing world at different timescales", *Atmosphere*, **13**, 1, 56.

Athira, K. S., Roxy, M. K., Dasgupta, P., Saranya, J. S., Singh, V. K. and Attada, R., 2023, "Regional and temporal variability of Indian summer monsoon rainfall in relation to El Niño southern oscillation", *Scientific Reports*, **13**, 1, 12643. https://doi.org/10.1038/s41598-023-38730-5

Beurs, K. M. D., Henebry, G. M., Owsley, B. C. and Sokolik, I. N., 2018, "Large scale climate oscillation impacts on temperature, precipitation and land surface phenology in Central Asia", *Environmental Research Letters*, **13**, 6, 065018.

Boschat, G., Terray, P. and Masson, S., 2012, "Robustness of SST teleconnections and precursory patterns associated with the Indian summer monsoon", *Climate dynamics*, **38**, 2143-2165. https://doi.org/10.1007/s00382-011-1100-7

Brandimarte, L., Di Baldassarre, G., Bruni, G., D'Odorico, P. and Montanari, A., 2011, "Relation between the North-Atlantic Oscillation and hydroclimatic conditions in Mediterranean areas", *Water Resources Management*, **25**, 1269-1279.

Chang, C. P., Harr, P. and Ju, J., 2001, "Possible roles of Atlantic circulations on the weakening Indian monsoon rainfall–ENSO relationship", *Journal of Climate*, **14**, 11, 2376-2380. https://doi.org/10.1175/1520-0442(2001)014<2376:PROACO>2.0.CO;2

Chattopadhyay, J. and Bhatla, R., 2002, "Possible influence of QBO on teleconnections relating Indian summer monsoon rainfall and sea-surface temperature anomalies across the equatorial pacific", *International Journal of Climatology: A Journal of the Royal Meteorological Society*, **22**, 1, 121-127. https://doi.org/10.1002/joc.661

Dehghani, M., Salehi, S., Mosavi, A., Nabipour, N., Shamshirband, S. and Ghamisi, P., 2020, "Spatial analysis of seasonal precipitation over Iran: Co-variation with climate indices", *ISPRS International Journal of Geo-Information*, **9**, 2, 73.

Feba, F., Ashok, K. and Ravichandran, M., 2019, "Role of changed Indo-Pacific atmospheric circulation in the recent disconnect between the Indian summer monsoon and ENSO", *Climate Dynamics*, **52**, 1461-1470. https://doi.org/10.1007/s00382-018-4207-2

Gadgil, S., Vinayachandran, P. N., Francis, P. A. and Gadgil, S., 2004, "Extremes of the Indian summer monsoon rainfall, ENSO and equatorial Indian Ocean oscillation", *Geophysical Research Letters*, **31**, 12. https://doi.org/10.1029/2004GL019733

Gao, T., Cao, F., Dan, L., Li, M., Gong, X. and Zhan, J., 2021, "The precipitation variability of the wet and dry season at the interannual and interdecadal scales over eastern China (1901–2016): the impacts of the Pacific Ocean", *Hydrology and Earth System Sciences*, **25**, 3, 1467-1481.

Ibebuchi, C. C., 2023, "Large-scale forcing over the homogeneous regions of summer rainfall anomalies in southern Africa", *Meteorological Applications*, **30**, 1, e2114.

Ihara, C., Kushnir, Y., Cane, M. A. and De La Peña, V. H., 2007, "Indian summer monsoon rainfall and its link with ENSO and Indian Ocean climate indices", *International Journal of Climatology: A Journal of the Royal Meteorological Society*, **27**, 2, 179-187. https://doi.org/10.1002/joc.1394

Ionita, M., 2014, "The impact of the East Atlantic/Western Russia pattern on the hydroclimatology of Europe from mid-winter to late spring", *Climate*, **2**, 4, 296-309.

Karumuri, A. and Saji, N. H., 2007, "On the impacts of ENSO and Indian Ocean dipole events on sub-regional Indian summer monsoon rainfall", *Natural Hazards*, **42**, 273-285. https://doi.org/10.1007/s11069-006-9091-0

Karumuri, A., Guan, Z. and Yamagata, T., 2001, "Impact of the Indian Ocean dipole on the relationship between the Indian monsoon rainfall and ENSO", *Geophysical research letters*, **28**, 23, 4499-4502. https://doi.org/10.1029/2001GL013294

Karumuri, A., Guan, Z. and Yamagata, T., 2003, "Influence of the Indian Ocean Dipole on the Australian winter rainfall", *Geophysical Research Letters*, **30**, 15.

Kavitha, S., Varuna, S. and Ramya, R., 2016, "A comparative analysis on linear regression and support vector regression", In 2016 online international conference on green engineering and technologies (IC-GET) (pp. 1-5). IEEE.

Li, G., Chang, W. and Yang, H., 2020, "A novel combined prediction model for monthly mean precipitation with error correction strategy", *IEEE Access*, **8**, 141432-141445. DOI:10.1109/ACCESS.2020.3013354

Maity, R. and Kumar, D. N., 2006, "Hydroclimatic association of the monthly summer monsoon rainfall over India with large-scale atmospheric circulations from tropical Pacific Ocean and the Indian Ocean region", *Atmospheric Science Letters*, **7**, 4, 101-107. https://doi.org/10.1002/asl.141

Maity, R., and Kumar, D. N. 2007, "Hydroclimatic teleconnection between global sea surface temperature and rainfall over India

at subdivisional monthly scale", *Hydrological Processes: An International Journal*, **21**, 14, 1802-1813. https://doi.org/10.1002/hyp.6300

Maity, R., Kumar, D. N. and Nanjundiah, R. S., 2007, "Review of hydroclimatic teleconnection between hydrologic variables and large-scale atmospheric circulation patterns with Indian perspective", *ISH Journal of Hydraulic Engineering*, **13**, 1, 77-92. https://doi.org/10.1080/09715010.2007.10514859

Marcella, M. P. and Eltahir, E. A. B., 2008, "The hydroclimatology of Kuwait: explaining the variability of rainfall at seasonal and interannual time scales", *Journal of hydrometeorology*, **9**, 5, 1095-1105.

Mishra, V., Smoliak, B. V., Lettenmaier, D. P. and Wallace, J. M., 2012, "A prominent pattern of year-to-year variability in Indian Summer Monsoon Rainfall", *Proceedings of the National Academy of Sciences*, **109**, 19, 7213-7217. https://doi.org/10.1073/pnas.1119150109

Najafi, H., Nourani, V., Sharghi, E., Roushangar, K. and Dąbrowska, D., 2022, "Application of Z-numbers to teleconnection modeling between monthly precipitation and large scale sea surface temperature", *Hydrology Research*, **53**, 1, 1-13. https://doi.org/10.2166/nh.2021.025

Najibi, N., Devineni, N. and Lu, M., 2017, "Hydroclimate drivers and atmospheric teleconnections of long duration floods: An application to large reservoirs in the Missouri River Basin", *Advances in water resources*, **100**, 153-167.

Peings, Y., Douville, H. and Terray, P., 2009, "Extended winter Pacific North America oscillation as a precursor of the Indian summer monsoon rainfall", *Geophysical research letters*, **36**, 11. https://doi.org/10.1029/2009GL038453

Rasouli, K., Scharold, K., Mahmood, T. H., Glenn, N. F. and Marks, D., 2020, "Linking hydrological variations at local scales to regional climate teleconnection patterns", *Hydrological Processes*, **34**, 26, 5624-5641.

Roy, I., Tedeschi, R. G. and Collins, M., 2019, "ENSO teleconnections to the Indian summer monsoon under changing climate", *International journal of climatology*, **39**, 6, 3031-3042. https://doi.org/10.1002/joc.5999

Sardana, D., Kumar, P. and Weller, E., 2022, "Seasonal extreme rainfall variability over India and its association with surface air temperature", *Theoretical and Applied Climatology*, 1-21. https://doi.org/10.1007/s00704-022-04045-0

Sehgal, V. and Sridhar, V., 2018, "Effect of hydroclimatological teleconnections on the watershed-scale drought predictability in the southeastern United States", *International Journal of Climatology*, **38**, e1139-e1157.

Sharma, P. J. and Teegavarapu, R. S., 2021, "Influences of local hydroclimatology and teleconnections on Florida's precipitation and temperature variability", *Hydrological Processes*, **35**, 9, e14347.

Singhania, A. K., Kale, G. D. and Borthakur, A. J., 2018, "Assessment of Circulation Indices Affecting Indian Summer Monsoon Rainfall, in Addition to ENSO and Equinoo", *Water Conservation Science and Engineering*, **3**, 2, 117-128. https://doi.org/10.1007/s41101-018-0046-6

Srivastava, A. K., Rajeevan, M. and Kulkarni, R., 2002, "Teleconnection of OLR and SST anomalies over Atlantic Ocean with Indian summer monsoon", *Geophysical research letters*, **29**, 8, 125-1. https://doi.org/10.1029/2001GL013837

Srivastava, G., Chakraborty, A. and Nanjundiah, R. S., 2019, "Multidecadal see-saw of the impact of ENSO on Indian and West African summer monsoon rainfall", *Climate Dynamics*, **52**, 6633-6649. https://doi.org/10.1007/s00382-018-4535-2

Yang, X. and Huang, P., 2021, "Restored relationship between ENSO and Indian summer monsoon rainfall around 1999/2000", *The Innovation*, **2**, 2. https://doi.org/10.1016/j.xinn.2021.100102